Caveats of non-linear fitting to brain tissue models of diffusion

Ileana O. Jelescu[1], Jelle Veraart[1], Els Fieremans[1], and Dmitry S. Novikov[1]

[1]*Center for Biomedical Imaging, Dept. of Radiology, NYU Langone Medical Center, New York, New York, United States*

Target audience: Biophysicists interested in advanced microstructural models of diffusion MRI (dMRI) in the brain.

Purpose: **To identify the sources of strong bias and uncertainty in nonlinear fitting of advanced diffusion models in the brain.** Compared to empirical DTI metrics, brain white/gray matter models[1-5] of diffusion come with the promise of improved specificity. However, in spite of the large number of *q*-space measurements compared to the number of model parameters, fit outputs suffer from bias and poor precision. Therefore most models employ strong simplifying assumptions, e.g. fixing some parameters to *a priori* values, for improved precision[3,5] at the expense of accuracy. In this work, we use the example of NODDI[5] (Neurite Orientation Dispersion and Density Index) to assess the behavior of non-linear fitting when all model parameters are free. We examine the landscape of the minimization problem defined by this family of models, and reveal the sources of bias and uncertainty in parameter estimation.

	Set #1	Set #2
f_{ic}	0.48	0.32
D_a	2.5	1.15
$D_{e\parallel}$	2.5	2.85
$D_{e\perp}$	1.3	1.1
κ / c_2	4.5 / 0.74	10.6 / 0.90

Table 1. Ground truth values for the two sets of combinations considered. Diffusivities are in μm^2/ms.

Methods: We use a ground truth dMRI signal $S = f_{ic} \int_{\mathbb{S}^2} f(\vec{n}) e^{-bD_a(\vec{q}\cdot\vec{n})^2} d\vec{n} + (1-f_{ic}) e^{-b\vec{q}^T\left(\int_{\mathbb{S}^2} f(\vec{n})\hat{D}_e(\vec{n})d\vec{n}\right)\vec{q}}$, where f is the fiber orientation distribution function (here, a Watson distribution characterized by the parameter κ), D_a is the intra-axonal diffusivity, $\hat{D}_e$ is the extra-axonal tensor with axial and radial diffusivities $D_{e,\parallel}$ and $D_{e,\perp}$, respectively, and f_{ic} is the intra-axonal water fraction. NODDI typically fixes $D_a = D_{e,\parallel} = 1.7$ μm^2/ms, and makes use of Archie's law, $D_{e,\perp} = D_{e,\parallel}(1\text{-}f_{ic})$, in order to obtain a precise fit of the neurite orientation dispersion (i.e., κ). Here, we release all diffusivity constraints. The simulated protocol consisted in one b=0 and two non-zero shells (b=1 and b=2 ms/μm^2) with 30 directions each. Two sets of ground truth values were used, collected in **Table 1**, which were designed to produce similar empirical DTI/DKI metrics (characteristic of human corpus callosum, ages 1-3), while representing very different scenarios. Set #1: $D_a = D_{e,\parallel}$ and $D_{e,\perp} = D_{e,\parallel}(1\text{-}f_{ic})$. Set #2: $D_a < D_{e,\parallel}$ and no particular tortuosity model assumed. We express the orientation dispersion as $c_2 \equiv \langle\cos^2\psi\rangle = 1/\left(2\sqrt{\kappa}\,F\right) - 1/(2\kappa)$, where $F = \sqrt{\pi}/2\, e^{-\kappa}\cdot \mathrm{erfi}\left(\sqrt{\kappa}\right)$. First, the 3-dimensional fitting landscape of each set was evaluated both in the absence and presence of noise (SNR = 50) by calculating the value of the objective function F_{obj} (sum of squares) for combinations of f_{ic}, D_a and κ, the remaining parameters taking their true value (**Table 1**). Second, for each set, the behavior of nonlinear fitting was tested by generating synthetic signal, both noiseless and with SNR = 50 and fitting it to the specified signal equation using a random initialization and a Levenberg-Marquardt algorithm with box constraints[6]. The procedure was repeated for 2500 different initializations and noise realizations. The starting point was randomly chosen from the parameter intervals: $0.2 \le f_{ic} \le 0.8$; $0.5 \le D_a, D_{e,\parallel} \le 3.0$; $0.1 \le D_{e,\perp} \le 2.0$; $1/3 \le c_2 \le 1$, with c_2 further converted into κ.

Results and discussion: The 3-dimensional landscape $F_{obj}(f_{ic}, D_a, \kappa)$ takes the form of a boomerang (Fig. 1), i.e. **a narrow pipe with a tight turn**. It can be shown that its shape is governed by the 2nd and 4th order moments and its shallowness by the 6th order moment of the signal. While the noiseless case shows that the global minimum is relatively well marked, the SNR=50 case shows that **noise makes the minimum extremely shallow**, with a very large vicinity along the pipe where the objective function has values nearly indistinguishable from that of the true minimum. This is a source of large uncertainty in parameter estimation and of spurious correlations between parameters. This boomerang shape also explains why the fitting algorithms are very sensitive to initialization: depending on which boomerang branch is first taken, the algorithm may not be able to take the sharp turn to explore the second branch, hence a potential source of bias. Furthermore, the full 5-dimensional landscape of $F_{obj}(f_{ic}, D_a, \kappa, D_{e,\parallel}, D_{e,\perp})$ is even more complex. The performance of nonlinear fitting in the full landscape is represented by histograms of fit results (Fig. 2). In the SNR=∞ case, for Set #1, the algorithm finds the ground truth in 98% of cases. For Set #2, there is a largely bi-modal behavior. The existence of two potential solutions means that, for $D_a < D_{e,\parallel}$, there is inherently a second combination with $D_a > D_{e,\parallel}$ to which the landscape is as favorable, and, depending on actual parameter values, both solutions might be physically plausible. This feature had been highlighted previously[7]. Practically speaking, this means that **in the 5-dimensional landscape, there are in fact not one, but two boomerangs**, hence an additional source of very strong bias. This bi-modality is levied for Set #1 where $D_a = D_{e,\parallel}$ and the two solutions are merged. While this scenario somewhat simplifies the fitting landscape, its use as an *a priori* model assumption needs biological validation. In the SNR=50 case, all histograms become extremely broad, with relatively flat distributions for D_a and $D_{e,\parallel}$. Therefore, in a realistic case of limited SNR, the non-linear fitting approach fails for such complex models, being highly dependent on algorithm initialization and noise realization.

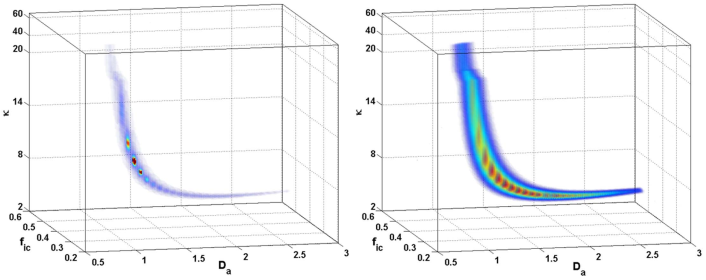

Figure 1. 3D representation of $F_{obj}(f_{ic}, D_a, \kappa)$ for Set #2, calculated for all combinations of: f_{ic}'s = 0.2:0.01:0.6; D_a's = 0.5:0.01:3.6; κ's = [2:0.1:20 21:1:64]. The color and transparency are function of $1/F_{obj}$, thus the global minimum is in red. The transparency feature reveals the existence of a narrow sharp-turning boomerang-shaped landscape of objective function values.

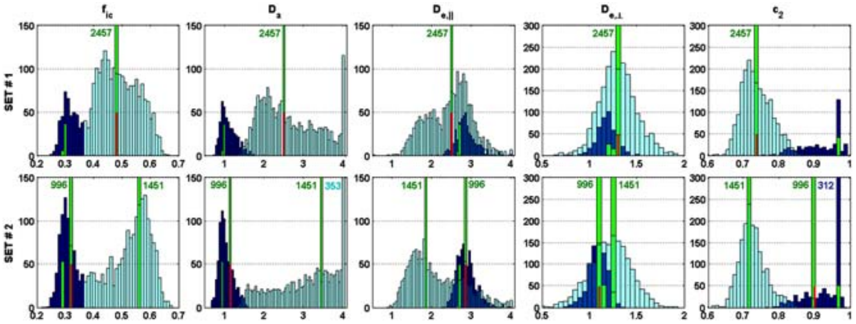

Figure 2. Histograms of fit results from 2500 random initializations and noise realizations for Sets #1 (top) and #2 (bottom). Red line: ground truth. Bright green histograms: SNR = ∞ (the actual counts are indicated beside the bar when it is taller than the display). For Set #2, there is a second solution ($f_{ic} = 0.56$ / $D_a = 3.44$ / $D_{e,\parallel} = 1.85$ / $D_{e,\perp} = 1.26$ / $c_2 = 0.72$) to the true one found with high frequency (58%). There is also another solution with low frequency (~2%), most likely the result of highly unfavorable initializations. Blue and cyan histograms: SNR = 50. The blue or cyan color was attributed based on the value of f_{ic} estimate, to visually separate two groups of solutions.

Conclusion: This study raises great concerns about the estimation of biophysical parameters using nonlinear fitting. The typical model of brain tissue with all features released cannot be reliably determined, due to an intrinsic duality of solutions, and to the narrow and shallow minimization landscape in SNR-limited cases. Constraining the fit using assumptions that so far lack biological validation is not a trustworthy solution to the problem.

References: [1] Behrens *et al.*, MRM 2003. [2] Kroenke *et al.*, MRM 2004. [3] Assaf *et al.*, MRM 2004. [4] Jespersen *et al.*, Neuroimage 2007. [5] Zhang *et al.*, Neuroimage 2012. [6] Lourakis, http://www.ics.forth.gr/~lourakis/levmar/+. [7] Fieremans *et al.*, Neuroimage 2011. Work supported by NIH R01 NS088040.